Journal of Food Engineering 320 (2022) 110928

Contents lists available at ScienceDirect

Journal of Food Engineering

journal homepage: www.elsevier.com/locate/jfoodeng

Research Article

Solute inclusion during progressive freeze concentration: A state diagram approach

Jan Eise Vuist, Maarten A.I. Schutyser [*,1], Remko M. Boom

Laboratory of Food Process Engineering, Wageningen University and Research, P.O. Box 17, 6700, AA, Wageningen, the Netherlands

ARTICLE INFO

Keywords:
Progressive freeze concentration
Solute inclusion
State diagram
Dewatering

ABSTRACT

We propose a conceptual model for progressive freeze concentration, which predicts solute loss through inclusion in the ice based on the system's phase behaviour as illustrated in a state diagram. We compare the outcomes of the model for sodium chloride, sucrose, and bovine serum albumin (BSA). For ice growth rates in the order 10^{-2} μm/s there was no solute inclusion for sodium chloride or sucrose, but above this range, local super-cooling gives rise to a freezing zone. In this freezing zone ice and solution co-exist and the resulting uneven advancement of the ice causes inclusions. The model predicts that for macromolecular solutions such as BSA, no inclusion will take place through the proposed mechanism.

1. Introduction

Freeze concentration is a mild process that involves the concentration of solutions by selective freezing of water. The process is typically used for the concentration of fruit juices, coffee extract, dairy products, and ice bock; all these products are susceptible to thermal degradation and benefit from the low temperatures in the process (Samsuri et al., 2016). Freeze concentration is also considered for the treatment of waste water (Holt, 1999), especially when these streams are corrosive, which can be reduced by the low temperature during the process.

Current freeze concentration process forms are suspension freeze concentration, block freeze concentration, and progressive freeze concentration (Sánchez et al., 2009, 2011). We here focus on progressive freeze concentration in which a layer of ice is created on the surface ofa heat exchanger. After the ice layer is grown, the concentrated solution is removed, the ice is melted and withdrawn from the system. This may be repeated multiple times to obtain a large enough concentration factor. Critical for the feasibility of this process is that the loss of solutes due to inclusion in the growing ice layer is minimised. These inclusions occur due to accumulation of solutes in the solution close to the ice growth front, which then induces uneven growth of the ice layer. Solute losses of up to 50% of the initial concentration can be found in the ice layer (Vuist et al., 2020, 2021; Jusoh et al., 2009; Ojeda et al., 2017). Depending on the amount of the inclusions and use of the ice fraction this can pose a significant loss of solutes.

The mechanism of solute inclusion during progressive freeze concentration in the growing ice layer is not yet completely unravelled. The phenomenon is generally understood to be caused by a temperature decrease in the boundary layer towards the ice interface. During ice growth, both water and heat are removed from the bulk solution, leading to an accumulation of solute on the ice surface, and a concurrent decrease in temperature in the boundary layer. Depending on the circumstances, the temperature in the boundary layer decreases below the freezing point of the local solution, which can then lead to ice growth from the surface, into the boundary layer (Fig. 1b). If the undercooling in the boundary layer is small, this may be seen as a ripple on the surface of the ice; but with increasing undercooling, dendritic ice crystals will be formed, which are surrounded by concentrated solution. During further growth of the ice layer, part of this concentrated solution gets included as pockets in the frozen ice layer.

The extent to which this inclusion takes place determines the effectiveness of the concentration of the solution. Jusoh et al. (2009) found experimentally that the overall experimental partition coefficient for glucose was relatively constant, when removing a similar amount of ice. Miyawaki et al. (1998) found that the distribution coefficient was dependent on the freezing rate and stirring rate. This led them to suggest a constant limiting distribution coefficient for a particular solute or solution. However, a simple consideration shows that this cannot be fundamentally valid. Ice growth at an infinitesimally slow freezing rate at the freezing temperature of the solution will avoid any accumulation of solutes before the ice, and therefore should result in pure ice. Thus, in

* Corresponding author.
E-mail address: maarten.schutyser@wur.nl (M.A.I. Schutyser).
[1] www.fpe.wur.nl (M.A.I. Schutyser).

https://doi.org/10.1016/j.jfoodeng.2021.110928
Received 4 May 2021; Received in revised form 8 December 2021; Accepted 28 December 2021
Available online 31 December 2021

Nomenclature

Subscripts

ice	Ice
b	Bulk
c	Composition path
f	Freezing point
i	Interface
m	Melting point

Symbols

Δh_f	Heat of fusion [J/mol]
δ	Thickness of boundary layer [m]
η	Cooling duty used for ice formation [%]
λ	Thermal conductivity [W/(m K)]
ρ	Density [kg/m^3]
b	Molality [mol/kg]
c	Concentration [M]
c_p	Heat capacity [J/kg]
D	Diffusion coefficient [m^2/s]
i	Van 't Hoff factor [−]
K	Instantaneous distribution coefficient [−]
k	Mass transfer coefficient [m/s]
K_f	Cryoscopic constant [(K kg)/mol]
N_{Nu}	Nusselt number [−]
N_{Pr}	Prandtl number [−]
N_{Re}	Reynold number [−]
N_{Sc}	Schmidt number [−]
N_{Sh}	Sherwood number [−]
q	Cooling duty [W/m^2]
T	Temperature [K]
v	Rate of water towards the interface/ice growth rate [m/s]
z	Coordinate [m]

this limiting case, the distribution coefficient will be zero. On the other hand, infinitely fast – or instantaneous – freezing will certainly lead to complete freezing of the solution, with just as much solute in the ice included, as was present in the original solution. In that case, the distribution coefficient will be one. Thus we conclude that the freezing rate influences the distribution coefficient: it varies at least with the rate of freezing, and it will therefore vary in time, as initially the freezing rate at the onset of the process will be large due to the absence of the ice film. Later in the process the freezing rate will drop, and thus the distribution coefficient will decrease. As indicated, previous research did not fully consider the impact of the dynamics on the inclusion behaviour of solutes, which is important for the effectiveness of this concentration method.

The aim of this study is therefore to offer an analysis to understand solute inclusion during progressive freeze concentration and how it is influenced by freezing point depression. For this we carry out a conceptual analysis of the freezing process, using state diagrams to visualize and analyse the process. We do this by constructing the trajectory of the solution through the state diagram while freezing, as function of the system parameters, and relative to the freezing curve in the state diagram. We consider the freeze concentration of three different types of solutes: NaCl as a representative of fast diffusing, low-molecular weight solutes; sucrose as a slower diffusing, intermediate molecular weight solute, and BSA as a representative of high molecular weight solutes. Finally, we extrapolate our findings towards even larger solutes, such as colloidal particles, which could for example be non-dissolved proteins.

2. Theory

2.1. State diagram

The freezing process takes place at the interface between the ice and the solution, assuming the presence of an initial ice layer that acts as a seed. The solute concentration on this surface is significant. Even if the solution itself has a limited solute concentration (say, a few percent), then the concentration polarization will result in much higher concentrations on the surface (Fig. 1). We therefore need to take freezing point depression into account; which is represented in a state diagram as a freezing curve with a negative slope.

The freezing point depression can be described with the Clausius-Clapeyron equation; but it is generally used with a constant enthalpy of fusion (Fellows, 2017). Since the enthalpy of fusion for water is quite dependent on the temperature, this leads to inaccurate description of the freezing curve in the state diagram; especially at higher solute concentration and hence lower freezing temperatures (Bertolini et al., 1985).

Therefore, we choose Blagden's law instead, which states that the freezing point of a solution is a in direct proportion to its concentration (Barrow, 1961):

$$T_m = T_m^0 - K_f \cdot b \cdot i \tag{1}$$

With K_f the cryoscopic constant (equal to 1.86 (Kkg)/mol), b the molality of the solution, and i the Van 't Hoff factor.

Fig. 2a shows for solutions of sucrose in water that while all descriptions are accurate for diluted solutions, Clausius-Clapeyron's equation deviates at lower temperatures and hence higher concentrations of sucrose. The established form of Blagden's law with $i = 1$, is just

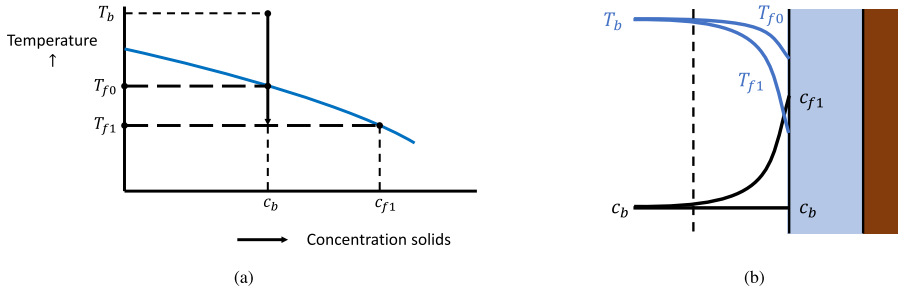

Fig. 1. Partial state diagram (a) and depiction of the concentrations and temperatures near the ice layer (b). At infinitesimally slow growth rates, there is no concentration polarization, indicated by subscript 0; at higher rates, there is concentration polarization and subsequently stronger freezing point depression at the ice surface, indicated by subscript 1 (Myerson et al., 2019).

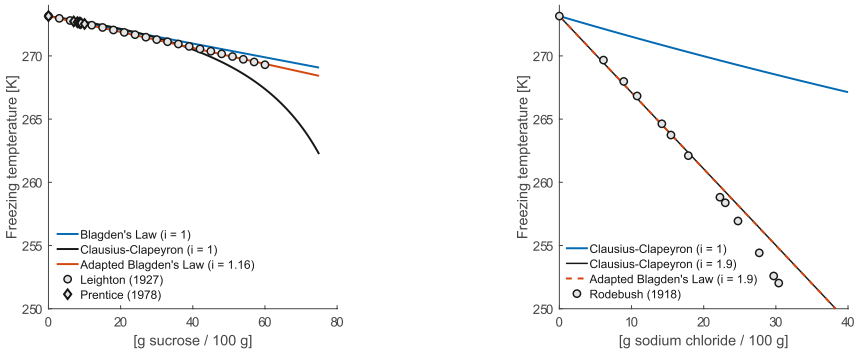

Fig. 2. Description of the freezing curve of sucrose-water solutions (a) and NaCl-water solutions (b) by Clausius-Clapeyron's equation using $\Delta h_f = 6001$ J/mol; and using Blagden's law. For sucrose lines are shown with $i = 1$ (blue line) and with $i = 1.16$ (red line). For NaCl solutions, lines are shown with $i = 1$, and with the generally assumed value of 1.9 (Leighton, 1927; Prentice, 1978; Rodebush, 1918). (For interpretation of the references to colour in this figure legend, the reader is referred to the Web version of this article.)

as accurate for diluted solutions, but deviates somewhat at higher concentrations. We adjusted this by assuming a Van 't Hoff factor of 1.16. One should regard this correction as merely a fit to take into account some nonideality of the solutions at higher concentrations. For NaCl solutions (Fig. 2b), we find that Clausius-Clapeyron and Blagden are identical, as long as $i = 1.9$ is taken for both descriptions.

The molecular weight of BSA is so large, i.e. 66.5 kDa, that the precise value of i is not very important. While a BSA molecule may have several counter-ions that would give rise of an i value that is clearly larger than one, for our considerations the freezing line for BSA is practically horizontal; therefore, we describe it with Blagden's law as well.

2.2. Concentration polarization and heat transfer

We now turn to the dynamics of the freeze concentration process. We assume that we extract heat from the system with a cooling duty or heat flow of q watts per m^2, through the layer of ice that has already formed. This heat is extracted by freezing water on the interface between ice and solution, and through heat extraction from the bulk of the solution. We assume that the bulk of the solution is well-mixed, with a boundary layer determining the rate of both heat and mass transfer to the interface.

First, we consider heat transfer through the boundary layer. If we assume an interface fixed frame of reference, heat transfer is through two modes, convective (transfer of water towards the interface, $v\rho c_p(T_b - T_i)$); and conductive ($-\lambda\frac{dT}{dz}$). Further, heat is released by freezing, ($v\rho\Delta h_f$), with v the rate of water towards the interface (m/s) and q is the cooling duty (Scholz et al., 1993):

$$v\rho c_p(T_b - T_i) - \lambda\frac{dT}{dz} + v\rho\Delta h_f = q \tag{2}$$

As the advective contribution is very small compared to the conductive and freezing contributions, we will neglect the first term. Using the heat transfer coefficient h, given by $h = \frac{\lambda}{\delta}$, with δ the thickness of the boundary layer, we get:

$$h(T_b - T_i) + v\rho\Delta h_f = q \tag{3}$$

The percentage of the cooling duty used for the formation of ice can be expressed as:

$$\eta = \frac{v\rho\Delta h_f}{q} \times 100\% \tag{4}$$

The heat transfer is found through a Nusselt relation, which may be of the form for flat plates under turbulent conditions:

$$N_{Nu} = 0.004\,3\ N_{Re}^{0.8}\ N_{Pr}^{0.33} \tag{5}$$

We then turn towards mass transfer, by considering the local concentrations of solute in the boundary later. Mass transfer through the same boundary layer can be described by:

$$vc - D\frac{dc}{dz} = vc_{ice} \qquad \text{or} \qquad \frac{dc}{dz} = \frac{v(c - c_{ice})}{D} \rightarrow \frac{c_i - c_{ice}}{c_b - c_{ice}} = \exp\left(\frac{v}{k}\right) \tag{6}$$

With the mass transfer coefficient $k = D/\delta$, found through a Sherwood relation, analogous to the Nusselt relation as it takes place through the same boundary layer:

$$N_{Sh} = 0.004\,3\ N_{Re}^{0.8}\ N_{Sc}^{0.33} \tag{7}$$

Both mass and heat transfer occur in the same boundary layer. That means that the compositions and temperatures in the boundary layer will form a curve, that starts at the point (c_b, T_b) and ends on the freezing curve at (c_i, T_i). Schematically, the curve could look as in Fig. 3.

We can calculate this curve more precisely by using both the temperature and the concentration gradients in the boundary layer to find the dependence of the temperature as function of the concentration (Chen et al., 2015).

$$\left.\begin{aligned} T_z &= T_i + (T_b - T_i)\frac{z}{\delta} \\ \frac{c_i - c_{ice}}{c_b - c_{ice}} &= exp\left(\frac{v(\delta - z)}{D}\right) \end{aligned}\right\} T_c = T_b - (T_b - T_i)\frac{k}{v}\ln\left(\frac{c_i - c_{ice}}{c_b - c_{ice}}\right) \tag{8}$$

In this relation, we do not yet know the concentration and temperature on the interface, c_i and T_i, and the concentration of solute in the ice, c_{ice}. We can find these by making use of the relations that we have. If we have solute inclusion, we can introduce the distribution coefficient $K = c_{ice}/c_b$, and thus eq. (8) can be rewritten in (Chen et al., 2015):

$$T_c = T_b - (T_b - T_i)\frac{k}{v}\ln\left(\frac{c_i - Kc_b}{c_b - Kc_b}\right) \tag{9}$$

We solve these eqs. (1), (3) and (9) for two distinct cases, in the first

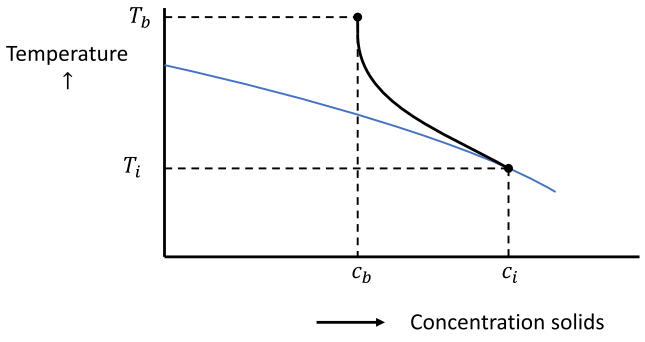

Fig. 3. Concentration profile in the boundary layer, starting at the bulk temperature and concentration, and ending on the solution-ice interface with concentration and temperature c_i, T_i.

case we assume slow freezing and that there is no inclusion, i.e. $c_{ice} = 0$ or $K = 0$. In the second case we assume that the freezing is faster and that there will be inclusions. The system of equations was solved using MathCad Prime (PTC Inc., USA; version 4.0).

2.3. Dynamics of slow freezing: no solute inclusion

In the case of very slow freezing, the ice inclusions will be zero, and thus $c_{ice} = 0$. In that case, it is straightforward to find the values of the parameters, see Fig. 4. We first set v, the freezing rate, as independent parameter, which will give us c_i through eq. (6) by taking $c_{ice} = 0$; then using eq. (1) with $T_m = T_i$, to find T_i, which can then be used to find $h(T_b - T_i)$ and therefore q using eq. (3) (Fig. 4c and f). In Fig. 4a and d the slow freezing is shown in the state diagram. The composition of the boundary layer does not cross the freezing line and therefore there won't be inclusions. If faster freezing is applied the composition in the boundary layer will cross the freezing line and a zone with super-cooling occurs in which solution and the tips of the ice crystals are present. This effect is also known as constitutional supercooling. In this case we need to invoke an extended model to account for the fast freezing (Fig. 4b and e).

The model also allows us to determine the concentration at the interface, c_i, and the minimum required cooling duty for ice growth (Fig. 4c and f). The concentration at the interface is useful information for to determine the maximum cooling duty to have no inclusions. This will be expanded upon in the next section. The minimum cooling duty arises from the heat flux for cooling down the bulk solution. This cooling down takes up part of the heat removed from the applied cooling duty (eq. (3)) and has to be overcome for the system to be able to form ice.

2.4. Dynamics of fast freezing: solute inclusion

If freezing is faster (induced by a larger temperature difference over the layer of ice), then the situation becomes different. The freezing front is stable, as long as the slope of the composition curve in the point (c_i, T_i) is larger (in absolute sense) than the slope of the freezing curve. In Fig. 5 we see an 'artist impression' of the situations.

At larger freezing rates (relative to the rate of diffusion of the solute), the concentration profile becomes steeper, and at some point it may cross the freezing curve (Fig. 5C). At this point, the solution within the boundary layer is below the freezing curve and therefore can freeze itself. One also can observe that the driving force for the formation of ice, which is the temperature difference between the local composition and the freezing curve, is smallest on the ice surface, and gets larger with the distance from the surface. That means, that any irregularity on the ice surface will have a larger driving force for freezing and therefore will grow faster than the ice surface on average. This means that there is a driving force for the ice to form oscillations, ultimately leading to the formation of needle-shaped, or dendritic ice crystals, from the surface, into the boundary layer, creating a freezing zone. The solution surrounding these ice crystals will become more and more concentrated and will ultimately be trapped into the ice, while the ice front will continue to move towards the bulk solution.

From a macroscopic standpoint, we observe that the ice incorporates a part of the solution, while the concentration polarization itself will become less extreme since a part of the solutes is not accumulating anymore in the boundary layer (Vuist et al., 2020, 2021). The situation as displayed in panel C of Fig. 5 will therefore relax with the situation in the boundary layer on the verge of instability.

The new situation, that results in zone freezing and solute inclusion,

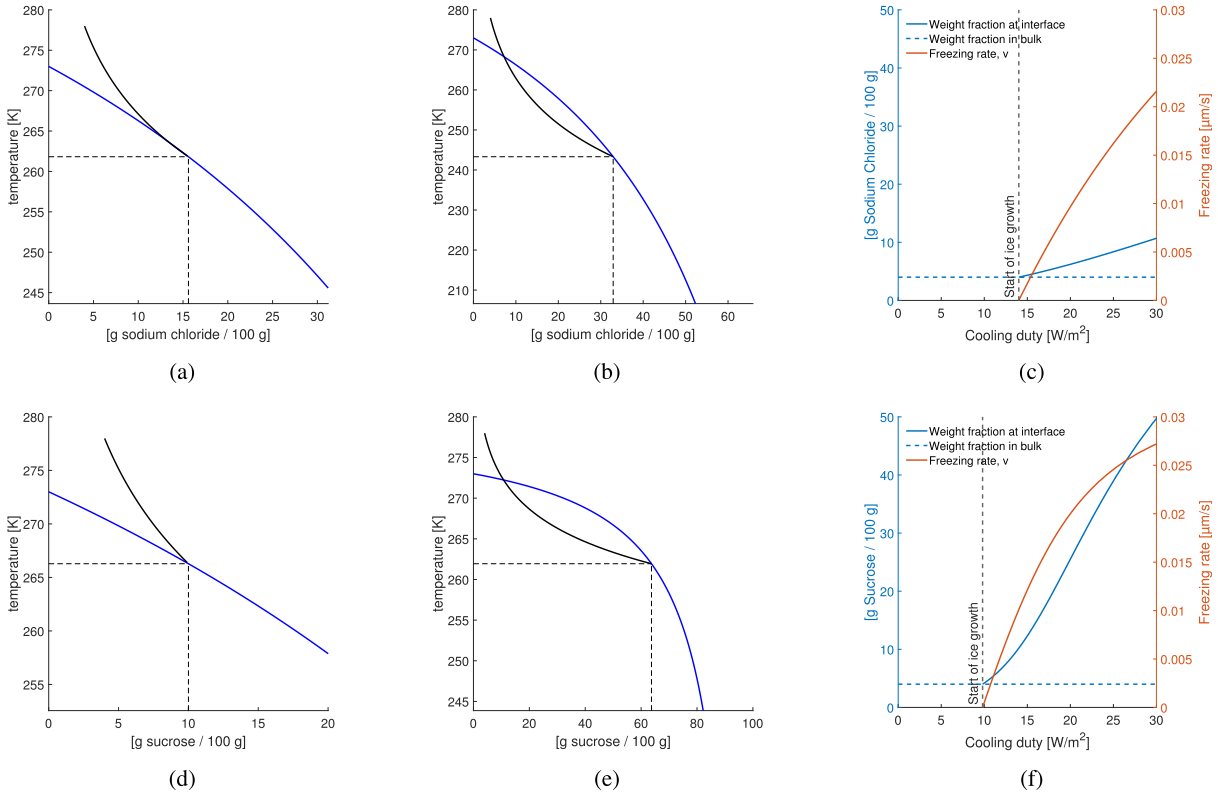

Fig. 4. (a) and (b) are state diagrams for sodium chloride with $q = 40$ W/m^2 (a) and with $q = 80$ W/m^2 (b). (d) and (e) are state diagrams for sucrose with $q = 20$ W/m^2 (d) and $q = 40$ W/m^2 (e). At (a) and (d), the freezing is stable. For the other situation, the composition in the boundary layer is unstable and will create a freezing zone in the boundary layer. The blue line represents the freezing line, the black line represents the temperature and composition in the boundary layer. The dashed lines indicate the temperature and composition at the interface. (c) sodium chloride and (f) sucrose, are plots of the freezing rate v and concentration at the interface c_i, as function of the cooling duty q. (For interpretation of the references to colour in this figure legend, the reader is referred to the Web version of this article.)

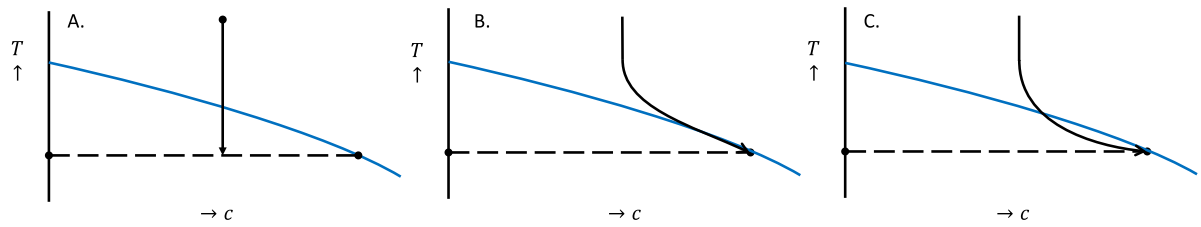

Fig. 5. Paths through the state diagram. A: before nucleation has started, a temperature gradient is created, but compositions have not yet changed. B: Slow freezing. The composition path stays outside the freezing line, and therefore the freezing front is stable. C: Fast freezing, resulting in ice formation in front of the freeze front and solute inclusion.

has one extra requirement, being that the slopes of the composition path and the freezing curve are the same (Tiller et al., 1953):

$$\frac{\mathrm{d}T_c}{\mathrm{d}c}_{(c_i,T_i)} = \frac{\mathrm{d}T_m}{\mathrm{d}c}_{(c_i,T_i)} \tag{10}$$

We can see in Fig. 6 that in the new situation the surface temperature goes up, and therefore we extract less heat from the solution; therefore more of the cooling is used to actually freeze water, albeit at lower purities. By simultaneously solving eqs. (1), (3) and (9) and applying boundary condition (10), we can find now the composition path that represents the compositions in the boundary layer that is now on top of the zone that undergoes dendritic (or similar) freezing. So, in this zone pure ice crystals and concentrated solution co-exist. When the freezing continues the freezing boundary will move into the direction of the solute and the ice crystals will overtake this mixed zone causing the solute inclusion. The distribution coefficient, K, is derived from eq. (9), since this the only unknown not determined by the other equations. Note in Fig. 6 that because the solution on top of the freezing zone has a higher temperature, this means that although we lose purification, we lose less heat through conduction from the bulk solution i.e. T_i at the top of the freezing zone is higher (eq. (3)). We typically see a sudden, slight reduction in overall energy duty necessary at this transition.

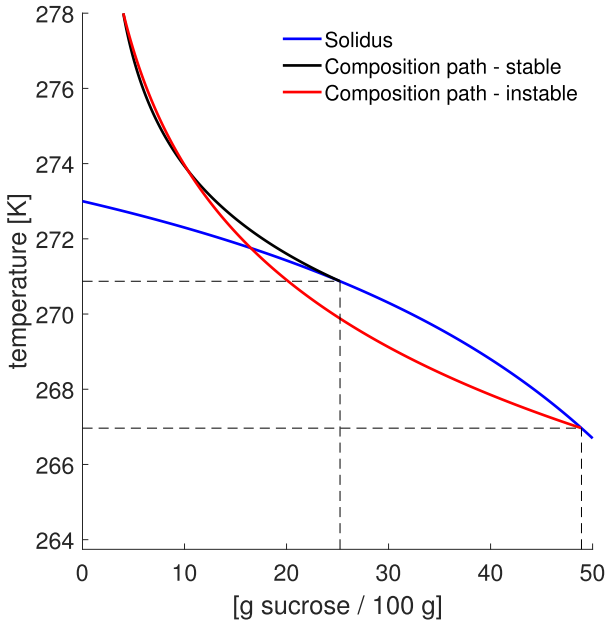

Fig. 6. Situation for a 4 w/w% solution of sucrose in water starting at 278 K, with 29.6 W/m^2 total heat removal duty. The blue curve is the freezing line. The red, unstable composition path gives rise to dendritic growth inside the boundary layer. The composition path for the boundary layer on top of the freezing zone, therefore relaxes to the verge of stability, indicated by the black curve. In this case we have a distribution coefficient of 0.49, meaning that the solute concentration in the ice is 49% of that in the bulk solution (which was 4% (w/w)) (eq. (9)). (For interpretation of the references to colour in this figure legend, the reader is referred to the Web version of this article.)

3. Results and discussion

3.1. Low-molecular weight solutions: NaCl-water and sucrose-water

Low molecular weight components such as NaCl and sucrose are abundant in food and other industrial streams. To not complicate the analyses, we neglect the temperature dependence of the parameters. These would change the quantitative outcomes, but not the qualitative ones. For a 4% (w/w) solution, we assumed that the diffusivity of NaCl in water is 1.5×10^{-9} m^2/s, and that of sucrose in water 5.2×10^{-10} m^2/s; and that the bulk solution was at 298 K. We also assumed that the thermal conductivity was constant at 0.561 0 W/(m K), and that the density of the solution remained at 1000 kg/m^3.

Both NaCl and sucrose give similar patterns as function of the freezing rate, with a stable freezing region below a certain cooling duty and freezing rates characterised by no inclusions, and unstable growth with increasing levels of inclusion above this threshold (Fig. 7). Due to the lower diffusion coefficients of sucrose in water, the transition occurs at a lower cooling duty with sucrose than with NaCl. During unstable freezing (and thus solute inclusion, the solute concentration on the interface between the freezing zone and the solution has a lower concentration and thus a higher temperature (dictated by the freezing line), and the amount of heat extracted from the bulk solution decreases at a higher rate again before levelling off (eq. (4)). At higher bulk concentrations the threshold between stable and unstable freezing will shift to lower freezing rates and therefore the process will be further limited, i.e. the maximally allowed cooling duty is lowered at higher concentrations. The threshold can be shifted to higher freezing rates if the Reynolds number goes up, i.e. if mixing in the bulk is improved.

It should be noted that the diffusivity of sucrose is in reality highly dependent on the temperature and concentration: since it is not too far off from the glass transition, it therefore follows Williams-Landel-Ferry kinetics, characterised by a much faster increase in viscosity and reduction in diffusivity than expected merely on basis of Arrhenius dependence (Kerr and Reid, 1994). The transition towards unstable freezing is therefore expected at even lower threshold values than indicated in Fig. 7. Difference between the two will therefore be much stronger in reality.

3.2. High-molecular weight solutions: proteins

While the principles are the same with high-molecular weight solutes, the state diagram dictates a somewhat different process. We here take the protein bovine serum albumin (BSA) as an example and calculated the composition paths during freeze concentration of BSA for different cooling duties (Fig. 8). The large molecular weight of the solute dictates a much more horizontal freezing line in the state diagram.

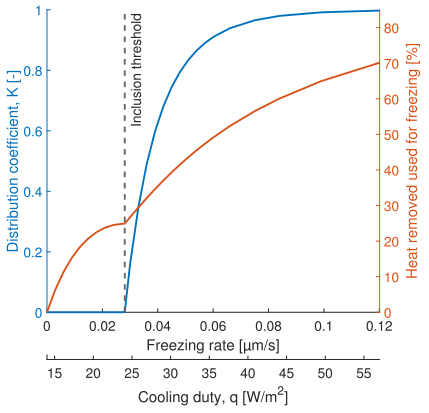

(a) NaCl-water

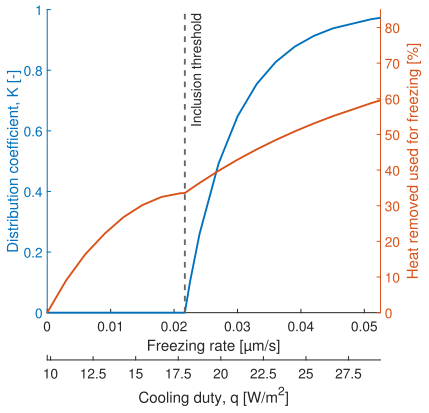

(b) sucrose-water

Fig. 7. Distribution coefficient K (blue line) and percentage of the cooling duty that is used for freezing of a 4% (w/w) solution (eq. (4), the rest is used for cooling the bulk solution; red line). Below the threshold, the composition paths are above the freezing line and freezing is stable. Above the threshold, a part of the profile is below the freezing line and distribution occurs, with an increasing value of the distribution coefficient, towards a value of 1 (implying no concentration at all). (For interpretation of the references to colour in this figure legend, the reader is referred to the Web version of this article.)

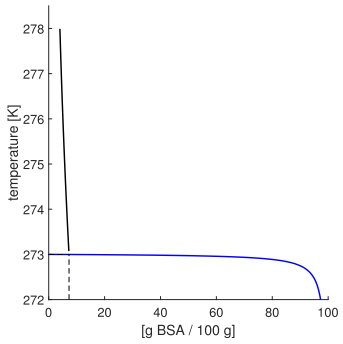

(a) $q = 9.82$ W/m^2

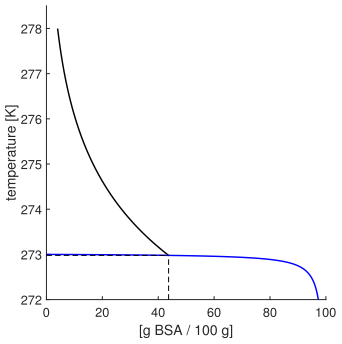

(b) $q = 11.36$ W/m^2

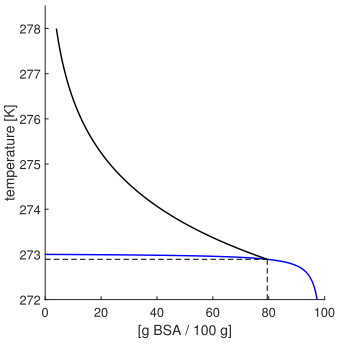

(c) $q = 12.02$ W/m^2

Fig. 8. Composition paths for a starting solution of 4% (w/w) BSA, for three different rates of heat extraction. The freezing line is so flat, that it is virtually impossible for the concentrations in the boundary layer to come below the freezing line. Surface concentrations are 7,3 (a), 43.7 (b) and 79.5 (c) % (w/w), respectively. The blue line represents the freezing line, the black line represents the temperature and composition in the boundary layer. (For interpretation of the references to colour in this figure legend, the reader is referred to the Web version of this article.)

Therefore, it is virtually impossible that the composition path in the boundary layer will get below the freezing line. Even at very high surface concentrations, the concentration polarization layer remains completely stable.

This means that for a high-molecular weight solute, no unstable freezing inside the concentration polarization layer will occur, and that solute inclusion according to the mechanism proposed is not possible. Of course, this is only valid as long as the solute remains in solution and does not precipitate.

It is known from the field of crossflow ultrafiltration, that concentration polarization of proteins on a membrane, at some point leads to the formation of a gel layer, in which the concentration of the protein is a constant (at equal temperature and solvent quality); often at around 0.6 kg/m^3 (Hiddink et al., 1980). We expect that this will also occur on top of an ice layer that extracts water from the solution and hence creates the same type of concentration polarization. Thus, at higher rates of heat extraction, a gel layer will form on top of the ice layer. This gel layer will also be stable (i.e. will not induce dentritic ice growth) but will form an insulating layer, reducing the mass and heat transfer, and thus reducing the rate of freezing. Therefore, we expect that at higher freezing rates, the rate of freezing will increase less than proportionally with the driving force for freezing. We can therefore predict that the protein concentration will remain stable, even at higher freezing rates.

This is only valid, as long as the freezing line has a very small, absolute, slope. This is the case when the solution contains only a high-molecular weight solute, but as soon as lower-molecular weight solutes are also present, then the freezing curve will have a larger, absolute, slope. At some point, the concentration in the polarization layer can cross the freezing line again, and cause unstable, dendritic ice growth in the boundary layer, and hence induce inclusion of both the low-molecular weight and the high-molecular weight solutes. We therefore predict that a solution containing both low-molecular and high-molecular weight solutes can result in solute inclusion again. So, unless the protein source is very pure, most realistic soluble protein solution will show solute inclusion in practice.

For proteins that are not dissolved at all but that are suspended as colloidal particles, we expect that the Brownian diffusivity of the particles is very small (Vuist et al., 2021). Even a very small amount of lower-molecular weight co-solutes will cause enough freezing point depression to allow these colloidal particles to be included. Therefore, we expect that for all practical conditions, undissolved components will be included in the ice.

3.3. Discussion on application of the theory

The results presented, are based on a highly simplified representation of the system. Diffusion and viscosity values were assumed to be constant and independent on the temperature. Of course, this is an oversimplification. A concentrated sucrose-water solution is anomalously viscous, since it is quite close to its glass transition. Such solutions exhibit Williams-Landel-Ferry kinetics, characterised by very sharp increases in viscosity with a reduction in temperature or an increase in

concentration. This implies that the local viscosity gradient for these solutions in the concentration polarization layer will be much steeper than assumed here. Similarly, the sucrose diffusion coefficient in water will be locally much lower in the concentration polarization layer, and hence the real concentration gradient will be much steeper. Therefore, the conclusions are only qualitative or at most semi-quantitative. The general behaviour that is found and described here, will however remain as is described. It is relatively straightforward to implement concentration and temperature dependence for the viscosity and diffusivities in the system, once these parameters are known with sufficient reliability in the relevant parameter space (temperature, composition).

Miyawaki et al. (1998) suggested that the inclusion factor be a constant. Later Gunathilake et al. (2013) observed that the inclusion factor is concentration dependent. One should bear in mind that experimental values for the inclusion factor are integrated over time, while the results shown here are only for momentary heat extraction rates. In a real process, the heat extraction at the beginning is very high, since there is no insulating ice layer formed yet on the heat exchanging surface, and will gradually decrease when the ice layer grows over time. At the beginning of the process, the inclusion rate will therefore be high, and will come down during the process. The experimentally measured inclusion factor is therefore a value that is integrated over time (Vuist et al., 2021). It is therefore expected that these integrated, experimental values are less variable than the momentary values, which are predicted in this work. Further elaboration of the model could certainly include the integration of the model over time.

4. Conclusions

It was shown that state diagrams can be useful to interpret the ice formation process during progressive freeze concentration. As long asthe composition path in the concentration polarization layer on top of the ice, does not cross the freezing line, freezing will be stable and unstable, dendritic ice formation inside the boundary layer is avoided. Instable ice formation inside the boundary layer will result in inclusion of solutes. This generally happens at larger ice formation rates, such that the concentration profile in the boundary layer becomes too steep, and in the state diagram, has a lower (absolute) slope than the freezing line. This prediction does not assume anything about the exact ice formation mechanism, and therefore, the phenomenon of solute inclusion therefore does not depend on whether the unstable ice formation in the boundary layer is dendritic or through any other type of growth mechanism.

We showed that inclusion of low-molecular weight solutes happens fairly quickly, due to the strong freezing point depression. The transition to unstable ice growth and solute inclusion happens at lower heat extraction rate with smaller molecules, larger absolute slope of the freezing line, and with slower-diffusing components, steeper concentration gradients. Solutions with only macromolecular solutes will not give any unstable ice growth, since the freezing line is virtually horizontal in the state diagram, not allowing the concentration gradient to cross the freezing line. We do expect however, that at some point, a gel layer will be formed on top of the ice, which will slow the formation of the ice. Solutions that contain both low-molecular weight and high-molecular weight components, will most probably show solute inclusion: the low-molecular weight components will give significant freezing point depression and a freezing line that has a larger absolute slope, while the macromolecular components have low diffusivities and hence will quickly accumulate on top of the growing ice layer.

The system was here strongly simplified by assuming viscosities and diffusivities to be independent on concentration and temperature. Inclusion of these effects will improve the quantitative accuracy of the model. Integration of the model over time will yield overall inclusion factors that can be more easily compared to experimental values.

The main application of this model is that it can be used to consider streams for progressive freeze concentration and to calculate their expected performance. Since the data needed for the estimation are easily measurable, an estimation of the expected performance can be made. This will save time and resources, which is especially valuable for scaling up progressive freeze concentration to a scale interesting for industrial application.

Credit author contribution statement

Jan Eise Vuist: Conceptualization, Methodology, Formal analysis, Writing – original draft preparation. Maarten A.I. Schutyser: Writing – original draft preparation, Funding acquisition. Remko M. Boom: Conceptualization, Writing – original draft preparation, Supervision.

Acknowledgements

This work is an Institute for Sustainable Process Technology (ISPT) project. Partners in this project are TNO, Royal Cosun, Nouryon, Wageningen University and ISPT. This project is co-funded with subsidy from the Topsector Energy by the Ministry of Economic Affairs and Climate Policy.

References

Barrow, G.M., 1961. Colligative properties of solutions. In: Physical Chemistry, chapter 15. McGraw-Hill, New York [etc.], pp. 499–503.

Bertolini, D., Cassettari, M., Salvetti, G., 1985. Anomalies in the "latent heat" of solidification of supercooled water. Chem. Phys. Lett. 119, 553–555. https://doi.org/10.1016/0009-2614(85)85387-2.

Chen, X.D., Wu, W.D., Chen, P., 2015. An analytical relationship of concentration-dependent interfacial solute distribution coefficient for aqueous layer freeze concentration. AIChE J. 61, 1334–1344. https://doi.org/10.1002/aic.14722.

Fellows, P.J., 2017. 20 – heat removal by refrigeration. In: Food Processing Technology, fourth ed. 2011, pp. 847–868. https://doi.org/10.1016/B978-0-08-100522-4.00020-1.

Gunathilake, M., Shimmura, K., Miyawaki, O., 2013. Analysis of solute distribution in ice formed in progressive freeze-concentration. Food Sci. Technol. Res. 19, 369–374. https://doi.org/10.3136/fstr.19.369. https://doi.org/10.3136/fstr.19.369.

Hiddink, J., de Boer, R., Nooy, P.F., 1980. Reverse osmosis of dairy liquids. J. Dairy Sci. 63, 204–214. https://doi.org/10.3168/jds.S0022-0302(80)82915-8.

Holt, S., 1999. The role of freeze concentration in waste water disposal. Filtrat. Separ. 36, 34–35. https://doi.org/10.1016/S0015-1882(00)80052-X. http://linkinghub.elsevier.com/retrieve/pii/S001518820080052X.

Jusoh, M., Yunus, R.M., Abu Hassan, M.A., 2009. Performance investigation on a new design for Progressive Freeze Concentration system. J. Appl. Sci. 9, 3171–3175. https://doi.org/10.3923/jas.2009.3171.3175. http://www.scialert.net/abstract/?doi=jas.2009.3171.3175.

Kerr, W.L., Reid, D.S., 1994. Temperature Dependence of the Viscosity of Sugar and Maltodextrin Solutions in Coexistence with Ice. https://doi.org/10.1006/fstl.1994.1046.

Leighton, A., 1927. Separation of cane sugar from water ice. J. Dairy Sci. 10, 219–223. https://doi.org/10.3168/jds.S0022-0302(27)93835-1. http://www.sciencedirect.com/science/article/pii/S0022030227938351.

Miyawaki, O., Liu, L., Nakamura, K., 1998. Effective partition constant of solute between ice and liquid phases in progressive freeze-concentration. J. Food Sci. 63, 4–6. https://doi.org/10.1111/j.1365-2621.1998.tb17893.x. https://doi.org/10.1111/j.1365-2621.1998.tb17893.x.

Myerson, A.S., Erdemir, D., Lee, A., 2019. Handbook of industrial crystallization. In: Handbook of Industrial Crystallization, third ed. ed. Cambridge University Press, Cambridge, pp. 266–289. https://doi.org/10.1017/9781139026949 (chapter 9). http://public.ebookcentral.proquest.com/choice/publicfullrecord.aspx?p=5928442. https://doi.org/10.1017/9781139026949.

Ojeda, A., Moreno, F.L., Ruiz, R.Y., Blanco, M., Raventós, M., Hernández, E., 2017. Effect of process parameters on the progressive freeze concentration of sucrose solutions. Chem. Eng. Commun. 204, 951–956. https://doi.org/10.1080/00986445.2017.1328413. https://doi.org/10.1080/00986445.2017.1328413.

Prentice, J.H., 1978. Freezing-point data on a aqueous solutions of sucrose and sodium chloride and the Horvart test: a reappraisal. Analyst 103, 1269–1273. https://doi.org/10.1039/AN9780301269. https://doi.org/10.1039/AN9780301269.

Rodebush, W.H., 1918. The freezing points OF concentrated solutions and the free energy OF solution OF salts. J. Am. Chem. Soc. 40, 1204–1213. https://doi.org/10.1021/ja02241a008. https://pubs.acs.org/doi/abs/10.1021/ja02241a008.

Samsuri, S., Amran, N.A., Yahya, N., Jusoh, M., 2016. Review on progressive freeze concentration designs. Chem. Eng. Commun. 203, 345–363. https://doi.org/10.1080/00986445.2014.999050. URL: http://www.tandfonline.com/doi/full/10.1080/00986445.2014.999050.

Sánchez, J., Hernández, E., Auleda, J.M., Raventós, M., 2011. Review: freeze concentration Technology applied to dairy products. Food Sci. Technol. Int. https://doi.org/10.1177/1082013210382479.

Sánchez, J., Ruiz, Y., Auleda, J.M., Hernández, E., Raventós, M., 2009. Review. Freeze concentration in the fruit juices industry. Food Sci. Technol. Int. 15, 303–315. https://doi.org/10.1177/1082013209344267. http://journals.sagepub.com/doi/abs/10.1177/1082013209344267.

Scholz, R., Wangnick, K., Ulrich, J., 1993. On the distribution and movement of impurities in crystalline layers in melt crystallization processes. J. Phys. Appl. Phys. 26, B156–B161. https://doi.org/10.1088/0022-3727/26/8B/025. http://stacks.iop.org/0022-3727/26/i=8B/a=025?key=crossref.a6f8fe8e0a886fd757698c1f69f83ab4.

Tiller, W.A., Jackson, K.A., Rutter, J.W., Chalmers, B., 1953. The redistribution of solute atoms during the solidification of metals. Acta Metall. 1, 428–437. https://doi.org/10.1016/0001-6160(53)90126-6.

Vuist, J.E., Boom, R.M., Schutyser, M.A.I., 2020. Solute inclusion and freezing rate during progressive freeze concentration of sucrose and maltodextrin solutions. Dry. Technol. 1–9 https://doi.org/10.1080/07373937.2020.1742151. https://www.tandfonline.com/doi/full/10.1080/07373937.2020.1742151.

Vuist, J.E., Linssen, R., Boom, R.M., Schutyser, M.A., 2021. Modelling ice growth and inclusion behaviour of sucrose and proteins during progressive freeze concentration. J. Food Eng. 303, 110592 https://doi.org/10.1016/j.jfoodeng.2021.110592. http://creativecommons.org/licenses/by/4.0/. https://linkinghub.elsevier.com/retrieve/pii/S0260877421001175.